First-principle prediction of single-carrier avalanche multiplication in chalcopyrite semiconductors

O. Rubel[1,2,a)] and A. Darbandi[1,2,3]
[1]*Thunder Bay Regional Research Institute, 290 Munro St., Thunder Bay, Ontario P7A 7T1, Canada*
[2]*Department of Physics, Lakehead University, 955 Oliver Road, Thunder Bay, Ontario P7B 5E1, Canada*
[3]*Department of Physics, Simon Fraser University, 8888 University Dr., Burnaby, BC V5A 1S6, Canada*

(Received 18 March 2013; accepted 9 May 2013; published online 23 May 2013)

A critical requirement for high gain and low noise avalanche photodiodes is the single-carrier avalanche multiplication. We propose that the single-carrier avalanche multiplication can be achieved in materials with a limited width of the valence band resulting in a restriction of kinetic energy for holes while allowing electrons to participate in the multiplication cascade. This feature of the electric structure is not common to the majority of technologically relevant semiconductors, but it can be anticipated in chalcopyrite $Cu(AlGa)Se_2$ alloys based on the presented electric structure calculations. © *2013 AIP Publishing LLC*. [http://dx.doi.org/10.1063/1.4807650]

I. INTRODUCTION

Impact ionization in semiconductors and subsequent avalanche multiplication of charge carriers is widely exploited in avalanche photodiodes (APDs), which have a wide range of applications as high-sensitivity photoreceptors.[1–3] APDs generally operate in a linear mode at a bias voltage lower than the breakdown voltage, where the output current is linearly proportional to the incident photon flux.[4] The requirements to semiconducting materials for linear APDs include high gain and low excess noise. In order to fulfill both requirements, semiconductors that feature a single-carrier type avalanche multiplication are needed.

Unfortunately, the disparity between impact ionization coefficients for electrons and holes (so-called *K*-factor or the impact ionization coefficient ratio) is far from its ideal value for the majority of technologically relevant semiconductors, such as Si, GaN, GaAs, (InGa)As, and InP.[5–11] It has been shown that the intrinsic multiplication noise can be further reduced (but not eliminated) by pseudograding the multiplication region with the materials of different ionization threshold energies forming a heterostructure.[12] Another extrinsic approach is to introduce an impurity band, which restricts the motion of hopping carriers while their counterparts contribute to impact ionization in a single carrier-type fashion.[13,14] Since the impurity band is shallow, this approach requires cooling the detector down to cryogenic temperatures.

Currently, only HgCdTe APDs clearly feature *intrinsic* single-carrier avalanche multiplication and exhibit a practically noiseless gain of the excess of 1000.[15,16] The composition-dependent tailorable energy band gap of the ternary (HgCd)Te alloy spans in the range of 2–10 μm, which makes this material system an attractive choice for infrared applications.[17] The exceptional characteristics of HgCdTe APDs with low cadmium content are due to exclusive impact ionization of electrons (so-called e-APD). However, in view of its low energy gap, the operation of HgCdTe APDs requires cooling down to 77–260 K in order to reduce the dark current[17] that makes this material system not suitable for room-temperature detectors.

Here, we propose the $CuAl_{1-x}Ga_xSe_2$ solid solution as a promising material system for room-temperature e-APDs. According to the electronic structure calculations, the intrinsic exclusive electron avalanche multiplication can be achieved in the $CuAl_{1-x}Ga_xSe_2$ alloy as a result of its peculiar valence band (VB) structure. It is a discontinuity in the density of valence states that precludes holes from gaining the excess energy required to produce a secondary electron-hole pair. This mechanism is notably different from that in HgCdTe alloys, where the exclusive avalanche multiplication of electrons is due to a drastic difference in the mobility of electrons and holes.[18]

II. PROPOSED BAND STRUCTURE

We begin with a discussion of a hypothetical electronic band structure for a material with exclusive electron avalanche. An example of such a band structure is shown in Fig. 1. Its characteristic feature is a limited width of the valence band, which prevents holes from gaining the excess energy equal or greater than the band gap E_g in order to initiate the impact ionization. In contrast to holes, electrons accelerated by the external electric field can span the energy range $E_k > E_g$ and thus initiate impact ionization. We anticipate the material with such an electronic structure to exhibit a full suppression of the counterpart carrier multiplication.

The band structure as in Fig. 1 is not common for the majority of technologically relevant group IV, III-V, and II-VI semiconductors. These materials usually have a wide valence band (much wider than E_g), and alternative mechanisms (other than those discussed in the preceding paragraph) determine the dominant type of charge carriers for avalanche multiplication. These mechanisms include the scattering due to phonons and alloy disorder,[19,20] but they do not provide an ultimate selectivity because of their nature. As a result, none of these semiconductors (except for

a)rubelo@tbh.net

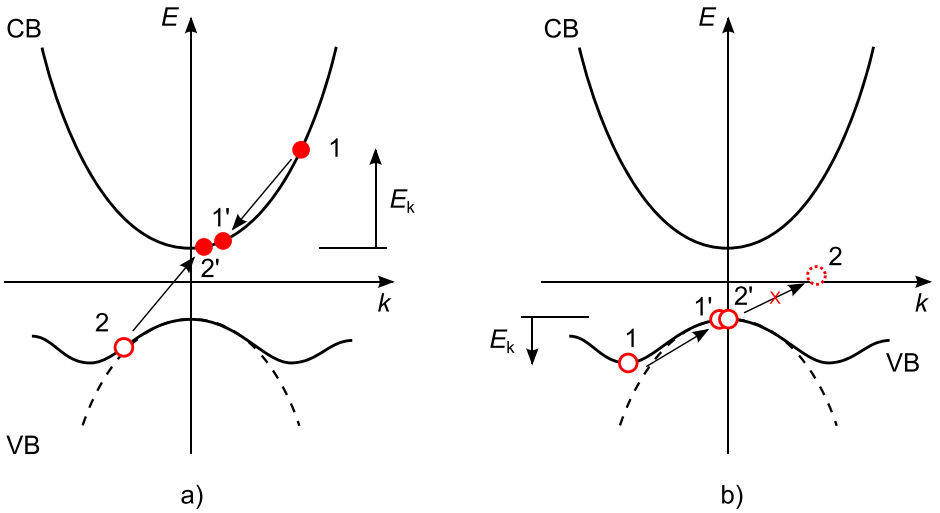

FIG. 1. Hypothetical band diagram of a material with single-carrier (electron) avalanche multiplication. The successful ionization event (a) is caused by the primary electron 1, which transfers its excess energy E_k to the electron 2 in the VB that results in creation of the secondary electron-hole pair 2–2′. The distinctive feature of this band structure is a limited width of the valence band (solid vs dashed line) that precludes holes (b) from gaining energy sufficiently high for the secondary electron-hole pair production.

HgCdTe) clearly feature single carrier type avalanche multiplication.

Engineering of materials with an intermediate band was targeted for photovoltaic applications due to an anticipated enhancement of the energy conversion efficiency.[21,22] This band was originally intended to provide an intermediate state for two-step photon absorption and designed to be semimetallic, which is not desired for our purpose.

It turns out that some ternary Ib-III-VI_2 chalcogenide semiconductors exhibit a narrow upper valence band,[23–26] which is well-separated from the rest of valence states. Ib-III-VI_2 semiconductors and their alloys were initially intended for LED applications as their compositional variation of the band gap can span the entire visible spectrum range. Currently, this material class is actively investigated as a low-cost alternative for thin-film solar cells.[27–29] However, to the best of our knowledge, the avalanche multiplication of metal-chalcogenide semiconductors is not explored yet. Next, we proceed with analysis of the electronic structure of $CuAlSe_2$.

III. RESULTS AND DISCUSSION

Under ambient conditions $CuAlSe_2$ crystalizes in a chalcopyrite structure shown in Fig. 2.[30] The band structure of $CuAlSe_2$ presented in Fig. 3(a) was calculated using a full-potential linearized augmented planewave implementation[31] of the density functional theory (details can be found in the Appendix). The distinct feature of this band structure is a relatively narrow (2 eV wide) top valence band separated by 1 eV gap from the rest of the valence states. This is what we refer to as the VB discontinuity (not to confuse with the band offset that occurs at a heterostructure interface). Since the optical band gap of $CuAlSe_2$ exceeds the width of the upper valence band, this material system is a suitable candidate for the exclusive electron avalanche multiplication. It is important to understand the origin of the VB discontinuity in Ib-III-VI_2 chalcogenide semiconductors and its sensitivity to the choice of chemical constituents.

The uppermost valence band and its discontinuity result from the hybridization between Cu-3*d* and Se-4*p* states[23,32] as shown in Fig. 3(c). Although the optical gap in $CuAlX_2$ compounds is sensitive to the choice of anion *X* (S, Se, or Te),[23] the valence band width and the VB gap appearance remain practically unchanged (compare Figs. 3(a) and 4(a)). This can be attributed to a little difference in the *p*-orbital energy between atomic chalcogens (Table I). As a result, the *p*-*d* hybridization and the VB structure are qualitatively identical for all $CuAlX_2$ compounds ($X = S$, Se, or Te).

On the other hand, the valence band in $AgAlSe_2$ (Fig. 4(b)) lacks the VB gap present in $CuAlSe_2$, which indicates its extreme sensitivity to the choice of transition element. This difference is due to the fact that Ag-4*d* electrons are energetically located *below* Se-4*p* electrons (Table I), which leads to switching the order of bands and a diminished *d*-character of the uppermost valence band.[32] Copper is the only group Ib transition element, whose *d*-orbital energy is *higher* than the *p*-orbital energy in chalcogens. Therefore, the presence of Cu is essential for the existence of the narrow top valence band.

The optical band gap of $CuAlSe_2$ is 2.67 eV (465 nm),[33] which makes this material an efficient absorber of blue and ultraviolet light. The question is whether it is possible to extend the sensitivity to longer wavelengths and span the

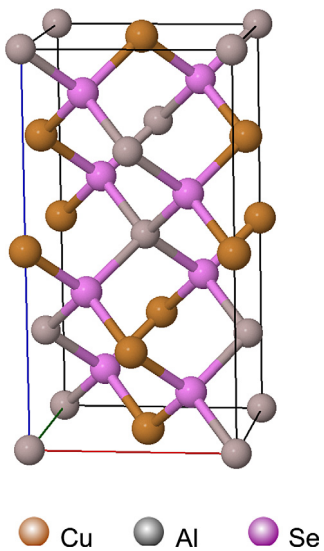

FIG. 2. Chalcopyrite structure of $CuAlSe_2$.

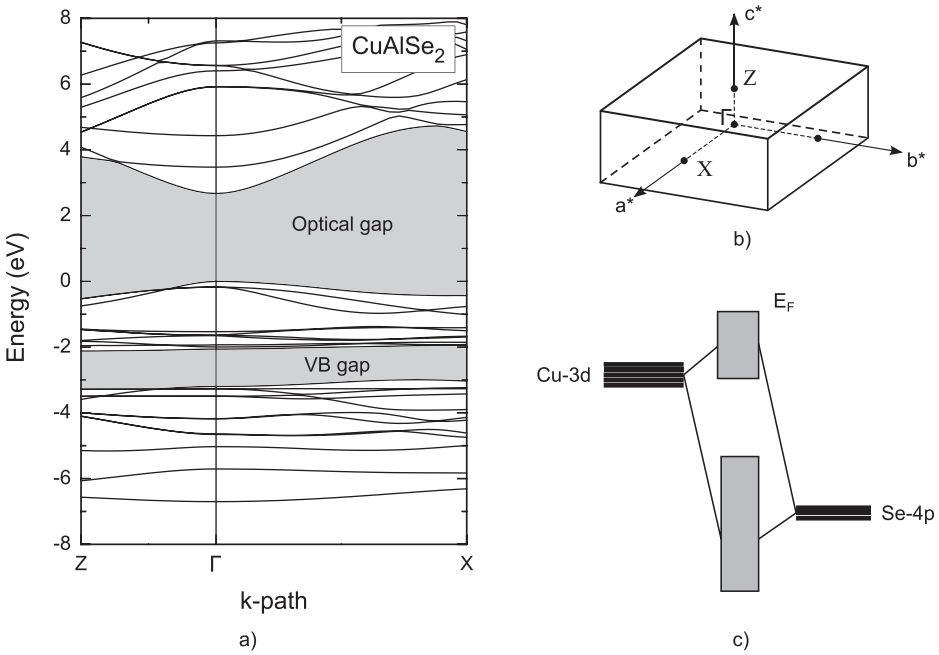

FIG. 3. Band structure (a) of the $CuAlSe_2$ chalcopyrite semiconductor plotted along the high-symmetry k-points in tetragonal Brillouin zone (b). The notable feature is a separation of the uppermost valance band from the rest of valance states. The energies are plotted relative to the Fermi energy E_F. The panel (c) illustrates p-d hybridization resulted in appearance of the VB gap.

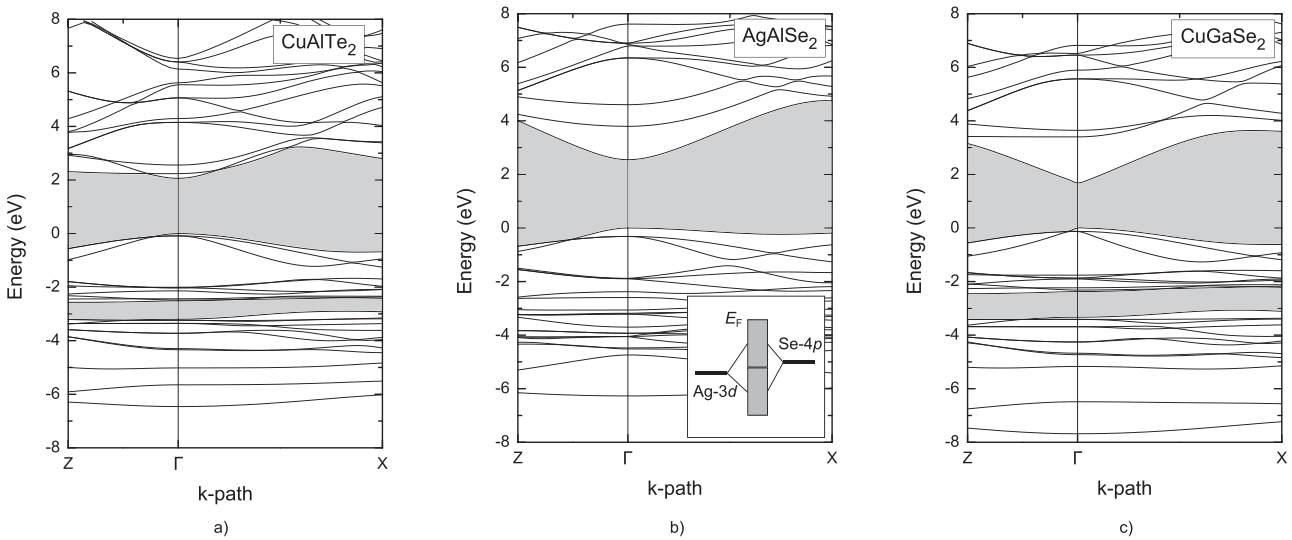

FIG. 4. Band structure of ternary chalcopyrite compounds. The notable feature is the separation of the uppermost valance band from the rest of valance states observed in $CuAlTe_2$ (a) and $CuGaSe_2$ (c), but not in $AgAlSe_2$ (b). The inset on panel (b) shows schematically the p-d hybridization in $AgAlSe_2$ that results in vanishing of the gap between bonding and antibonding states forming the upper VB. The energies are plotted relative to the Fermi energy E_F.

visible spectrum by manipulating the optical energy gap (e.g., via alloying) without distorting the valence band discontinuity. Reduction of the energy gap has also another benefit. It should lower the threshold electric field, which corresponds to the onset of impact ionization. Lowering of the energy gap can be achieved in a solid solution formed by isoelectronic substitution (typically with higher atomic number elements) at either group-III or group-VI sublattices.

One possible scenario is to form a quaternary alloy $CuAlSe_{2(1-y)}Te_{2y}$. However, a large discrepancy between

TABLE I. Energies (eV) of valence atomic orbitals for selected elements obtained with a relativistic local spin density approximation. The values in numerator and denominator correspond to the electron spin up/down.

Orbital	Cu	Ag	Al	Ga	Se	Te
$d_{3/2}$	−5.5/−5.4	−8.1/−7.9	…	−19.6/−19.5	…	…
$d_{5/2}$	−5.2/−5.1	−7.5/−7.3	…	−19.1/−19.0	…	…
$s_{1/2}$	−5.2/…	−5.0/…	−8.1/−7.4	−9.3/−8.8	−18.0/−16.6	−15.6/−14.6
$p_{1/2}$	…	…	−3.0/…	−3.0/…	−7.4/−6.1	−7.0/−6.0
$p_{3/2}$	…	…	…	…	−7.0/…	−6.2/…

covalent radii of Se and Te (1.22 vs 1.47 Å, respectively[34]) will result in local lattice distortions and, consequently, a limited solubility of Te in $CuAlSe_2$. The alternative approach is the isoelectronic substitution at the group-III sublattice. Gallium is the most favorable candidate based on the covalent radii argument (1.22 vs 1.21 Å for Ga and Al, respectively[34]). Consequently, there is no limit in solubility for $CuAl_{1-x}Ga_xSe_2$ alloys,[35] which provides an opportunity to span the entire visible spectrum range. In our case, however, we set the upper limit for Ga content at $x \leq 0.45$ in order to ensure that the width of the top valence band $W_{VB} \approx 2.1$ eV does not exceed the optical energy gap of the solid solution, the composition dependence of which is reported in Ref. 33.

In order to show that alloying does not affect the VB discontinuity, we performed the electronic structure calculation of $CuAl_{0.55}Ga_{0.45}Se_2$ solid solution. Due to the finite size of a supercell (64 atoms), the following stoichiometry $Cu_{16}Al_9Ga_7Se_{32}$ was chosen to represent the alloy. Aluminum and gallium atoms were randomly distributed on the group-III sublattice that resulted in the structure shown in Fig. 5. The corresponding band structure of such an alloy is shown in Fig. 6. The calculations confirm the presence of VB discontinuity in the $CuAl_{1-x}Ga_xSe_2$ solid solution. Furthermore, the width W_{VB} remains practically unchanged in comparison to the original band structure of $CuAlSe_2$ (Fig. 3).

An analysis of a projected density of states (DOS) shown in Fig. 7 provides further inside to the contribution of individual atoms to the total DOS of the $CuAl_{0.55}Ga_{0.45}Se_2$ alloy. As one can see, Cu-*d* with an admixture of Se-*p* electrons dominate in the uppermost VB as the antibonding states resulting from *p-d* hybridization. Their bonding counterpart is located approximately 3–6 eV below the Fermi energy.

The hybridization between the group-III metal *s*-states and Se-*p* states creates a narrow *s*-like bonding states with the energy of approximately 6–8 eV below the Fermi energy (Fig. 7). The corresponding antibonding states constitute the conduction band minimum.[36] Therefore, we expect the alloy disorder in $CuAl_{1-x}Ga_xSe_2$ to reflect primarily on the conduction band. Decreasing of the optical energy gap with

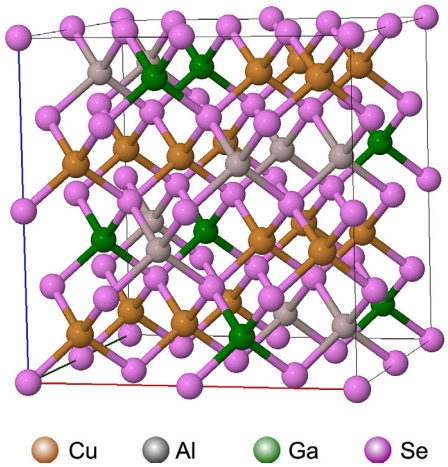

FIG. 5. Structure of the $Cu_{16}Al_9Ga_7Se_{32}$ random alloy.

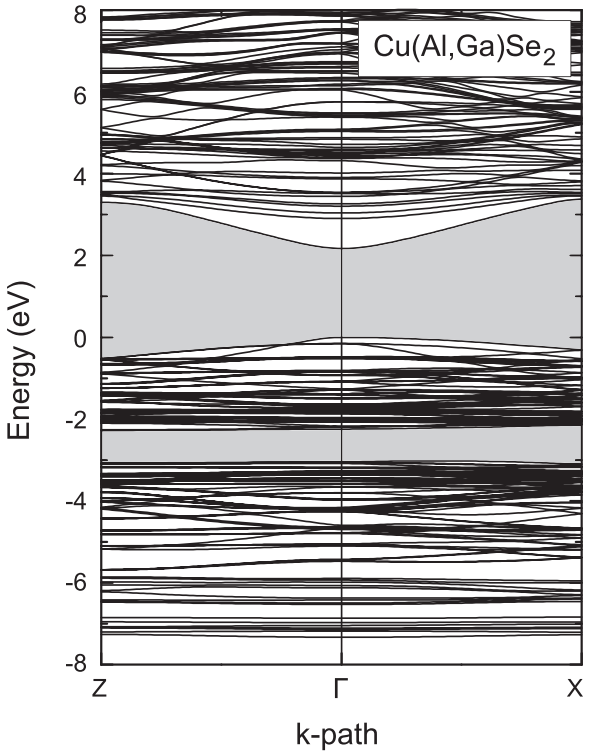

FIG. 6. Band structure of $Cu_{16}Al_9Ga_7Se_{32}$ random alloy plotted relative to the Fermi energy.

increasing Ga content in the $CuAl_{1-x}Ga_xSe_2$ alloy can then be attributed to the fact that Ga-s* antibonding states are located energetically below Al-s* states. At the same time, the VB discontinuity remains throughout the entire composition range *x*.

Next, we would like to comment on other material parameters that determine feasibility of avalanche multiplication. The simplest model of avalanche multiplication in crystalline semiconductors was proposed by Baraff[37] and further advanced by Ridley[38] and Burt.[39] The key parameters include the ionization energy threshold, the optical phonon energy, and the mean free path for carrier scattering due to optical phonons.

The ionization energy threshold E_i can be calculated using a detailed band structure in the full Brillouin zone.[40,41] The allowed transitions are determined taking into account both energy and momentum conservation requirements. Our calculations yield $E_i = 3.0$ eV for $CuAlSe_2$, which are significantly lower than the result anticipated from the parabolic band approximation $E_i = 3E_g/2 = 4.0$ eV.[42] The lower threshold energy is a favorable factor for impart ionization. The discrepancy between E_i values can be largely attributed to the limited dispersion $E(k)$ of holes, which manifests in a large discrepancy of effective masses for holes and electrons $m_h^* \sim 10m_e^*$.[26] This property is related to the localized *d*-character of the upper valence band, and it is inherent to all chalcopyrite semiconductors, including $CuAlSe_2$ (Fig. 3(a)).

Measurements of transport coefficients in $CuAlSe_2$ indicate that the room-temperature electron mobility varies in the broad range of 35–295 $cm^2 V^{-1} s^{-1}$.[43–46] The variation is attributed to extrinsic factors (defects and/or impurities).[46]

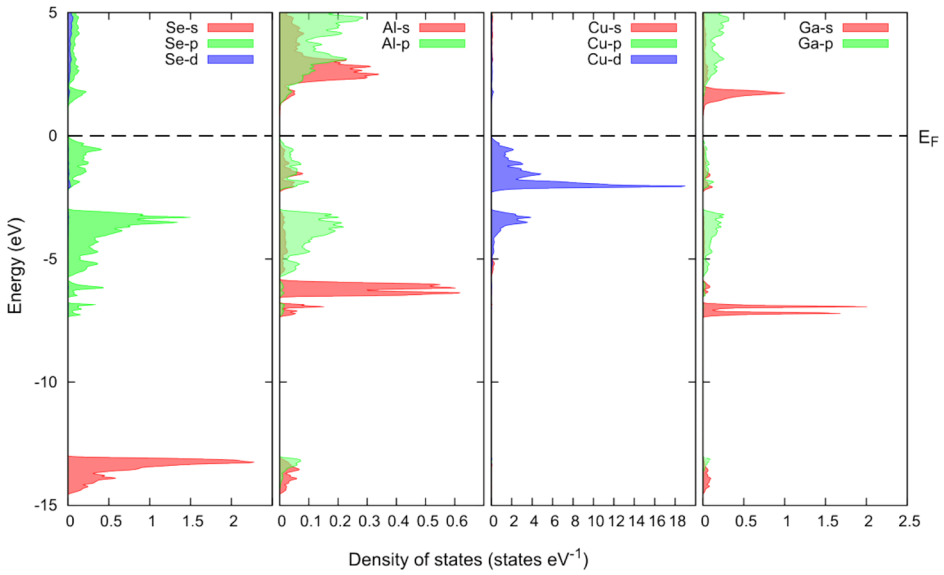

FIG. 7. Atom-specific projected density of states for the $Cu_{16}Al_9Ga_7Se_{32}$ random alloy.

The high-temperature mobility tends to decrease as a function of $T^{-3/2}$ that is indicative of the thermal carrier scattering due to acoustic phonons.[46] In the case of hot carriers, the optical phonon interaction will likely become the dominant scattering and energy loss mechanism,[37,47] but there is not enough data to estimate the value of the optical phonon mean free path in $CuAlSe_2$. We can only refer to the optical phonon energy, which amounts to 50 meV in $CuAlSe_2$ (Ref. 48) that is less than the corresponding value in Si (60 meV (Ref. 49)).

Finally, we would like to discuss a possible APD device structure based on the standard p–i–n configuration (Ref. 50, p. 689). The proposed architecture is shown in Fig. 8. It is expected to provide high quantum efficiency and low noise, due to separation of the absorption and multiplication regions. The high value of absorption coefficient $\alpha \gtrsim 10^4$ cm^{-1} inherent to I–III–VI_2 chalcopyrite semiconductors[51–53] suggests that the thickness of the absorption p^+ region should not exceed 1 μm. The thickness of the multiplication i region should be determined empirically depending on the electric field, targeted multiplication factor, and the electron impact ionization coefficient of $Cu(AlGa)Se_2$.

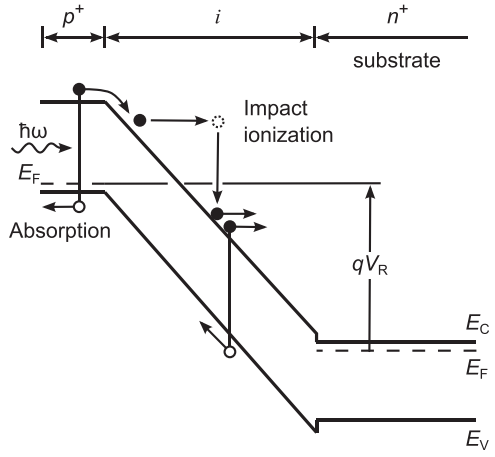

FIG. 8. Proposed device structure and energy-band diagram of $Cu(AlGa)Se_2$ APD under a reverse bias V_R.

The p-type conductivity can be readily achieved in $CuAlSe_2$ and $CuGaSe_2$ compounds.[54,55] In spite of some isolated successful attempts,[44,56] n-type conductivity is not systematically achieved in wide bandgap Cu–III–VI_2 semiconductors[57,58] due to the spontaneous formation of Cu vacancies that causes self-compensation as the Fermi level approaches the conduction band.[59,60] This property precludes realization of a homojunction APD structure. Alternatively, n-type GaAs or GaP can be used as the substrate. Successful growth of such heterostructures has been reported earlier.[61,62] The choice of GaAs is preferred since it forms type-I heterointerface with $CuAlSe_2$ and $CuGaSe_2$ (Ref. 63) that ensures barrier-free transport of electrons.

IV. CONCLUSION

Here, we proposed a band structure that favors single carrier avalanche multiplication. The distinct feature of this band structure is a limited width ($W_{VB} < E_g$) of the upper valence band that constrains holes from acquiring enough excess energy and thus limits their participation in the avalanche multiplication. It is proposed that such a peculiar band structure can be realized in Cu-based chalcopyrite semiconductors, such as $CuAl_{1-x}Ga_xSe_2$ solid solution ($x \leq 0.45$) with the optical energy gap within the visible spectrum. This hypothesis is supported by first-principle electronic structure calculations of ternary and quaternary chalcopyrite structures. It is shown that the energetic position of Cu-3d states located *above* the anion p-states is the critical factor for achieving a narrow upper valence band being isolated from the rest of valence states. This work opens an avenue for development of room-temperature low-noise avalanche photodetectors with a tailored band gap in the visible spectrum range.

ACKNOWLEDGMENTS

Financial support of Natural Sciences and Engineering Research Council of Canada under a Discovery Grants Program "Microscopic theory of high-field transport in disordered semiconductors" is highly acknowledged.

TABLE II. Lattice parameters a and c (Å) and the optical energy gap E_g (eV) of chalcopyrite compounds studied here.

Compound	a	c	E_g	Reference
$CuAlSe_2$	5.606	10.90	2.67	33 and 67
$CuAlTe_2$	5.964	11.78	2.06	67 and 68
$AgAlSe_2$	5.956	10.75	2.55	67 and 68
$CuGaSe_2$	5.607	10.99	1.68	33 and 67
$CuAl_{0.56}Ga_{0.44}Se_2$	5.606	10.94[a]	2.17	33

[a]The result is obtained by a linear interpolation between $CuAlSe_2$ and $CuGaSe_2$ ternary compounds.

APPENDIX: ELECTRONIC STRUCTURE CALCULATION METHOD

The electronic structure calculations were undertaken using a density functional theory (DFT) in the framework of the full-potential linearized augmented plane wave method, which is implemented in WIEN2K package.[31] The simulation cell volume was partitioned onto non-overlapping spheres centred at the nucleus of individual atoms with an interstitial region between them. The following radii of $R_{MT} = 1.9$, 2.05, 2.05, 2.05, 2.15, and 2.15 Bohr were assigned to Se, Te, Al, Ga, Cu, and Ag, respectively. The product of the atomic sphere radius and of the plane wave cut-off k-vector (the so-called RK_{max} parameter) was equal to 7 for all structures. The local density approximation (Perdew and Wang[64] parametrization) was employed for the exchange-correlation functional. The energy needed to separate core and valence electrons was set to −6 Ry, which results in treating of semi-core d-electrons as valence electrons in Cu, Ag, Ga, Se, and Te. The Brillouin zone of a tetragonal body-centred primitive unit cell was sampled using a shifted $8 \times 8 \times 8$ Monkhorst-Pack[65] k-point mesh.

Calculations were performed at the experimental values of the lattice parameters listed in Table II. Optimization of internal degrees of freedom was performed for all structures. The structural optimization was continued until the Hellmann-Feynman forces acting on the atoms reached the value of 2 mRy/Bohr or lower. DFT systematically underestimates the optical energy gap for calculated structures. This inconsistency is attributed to a well-known shortcoming of explicit density-dependent functionals, which tend to underestimate the energy gap.[66] In Figs. 3–7 and the following analysis, the so-called "scissor operator" (energy offset) was applied in order to match the theoretical energy gap with its experimental value (Table II).

[1]J. Campbell, J. Lightwave Technol. **25**, 109 (2007).
[2]J. David and C. Tan, IEEE J. Sel. Top. Quantum Electron. **14**, 998 (2008).
[3]R. Lecomte, J. Cadorette, S. Rodrigue, D. Lapointe, D. Rouleau, M. Bentourkia, R. Yao, and P. Msaki, IEEE Trans. Nucl. Sci. **43**, 1952 (1996).
[4]T. Yoshizawa, *Handbook of Optical Metrology: Principles and Applications* (CRC Press, 2009), Vol. 10.
[5]S. Kasap, C. Koughia, H. Ruda, and R. Johanson, "Electrical conduction in metals and semiconductors," *Springer Handbook of Electronic and Photonic Materials* (Springer, 2006), pp. 19–45.
[6]*GaAs and Related Materials*, edited by S. Adach (World Scientific Publishing Co., Singapore, 1994).
[7]Y.-J. Yu, G. Bosman, and P. K. Bhattacharya, Appl. Phys. Lett. **51**, 1433 (1987).
[8]L. W. Cook, G. E. Bulman, and G. E. Stillman, Appl. Phys. Lett. **40**, 589 (1982).
[9]R. McClintock, J. L. Pau, K. Minder, C. Bayram, P. Kung, and M. Razeghi, Appl. Phys. Lett. **90**, 141112 (2007).
[10]I. H. Oguzman, E. Bellotti, K. F. Brennan, J. Kolník, R. Wang, and P. P. Ruden, J. Appl. Phys. **81**, 7827 (1997).
[11]X. Wang, W. Hu, X. Chen, J. Xu, L. Wang, X. Li, and W. Lu, J. Phys. D: Appl. Phys. **44**, 405102 (2011).
[12]S. Wang, R. Sidhu, X. G. Zheng, X. Li, X. Sun, A. L. Holmes, and J. C. Campbell, IEEE Photonics Technol. Lett. **13**, 1346 (2001).
[13]M. D. Petroff, M. G. Stapelbroek, and W. A. Kleinhans, Appl. Phys. Lett. **51**, 406 (1987).
[14]F. Szmulowicz and F. L. Madarasz, J. Appl. Phys. **62**, 2533 (1987).
[15]M. Kinch, J. Beck, C. Wan, F. Ma, and J. Campbell, J. Electron. Mater. **33**, 630 (2004).
[16]J. Beck, C. Wan, M. Kinch, J. Robinson, P. Mitra, R. Scritchfield, F. Ma, and J. Campbell, J. Electron. Mater. **35**, 1166 (2006).
[17]A. Rogalski, Infrared Phys. Technol. **54**, 136 (2011).
[18]F. Bertazzi, M. Moresco, M. Penna, M. Goano, and E. Bellotti, J. Electron. Mater. **39**, 912 (2010).
[19]E. Bellotti and F. Bertazzi, J. Appl. Phys. **111**, 103711 (2012).
[20]A. Darbandi and O. Rubel, J. Non-Cryst. Solids **358**, 2434 (2012).
[21]A. Luque and A. Martí, Phys. Rev. Lett. **78**, 5014 (1997).
[22]D. F. Marrón, A. Martí, and A. Luque, Thin Solid Films **517**, 2452 (2009).
[23]J. E. Jaffe and A. Zunger, Phys. Rev. B **29**, 1882 (1984).
[24]S. Laksari, A. Chahed, N. Abbouni, O. Benhelal, and B. Abbar, Comp. Mater. Sci. **38**, 223 (2006).
[25]A. Soni, V. Gupta, C. M. Arora, A. Dashora, and B. L. Ahuja, Sol. Energy **84**, 1481 (2010).
[26]I. Aguilera, J. Vidal, P. Wahnón, L. Reining, and S. Botti, Phys. Rev. B **84**, 085145 (2011).
[27]B. J. Stanbery, Crit. Rev. Solid State Mater. Sci. **27**, 73 (2002).
[28]W. Wang, Y.-W. Su, and C. h. Chang, Sol. Energy Mater. Sol. Cells **95**, 2616 (2011).
[29]L.-J. Chen, J.-D. Liao, Y.-J. Chuang, and Y.-S. Fu, J. Am. Chem. Soc. **133**, 3704 (2011).
[30]R. S. Kumar, A. Sekar, N. Jaya, S. Natarajan, and S. Chichibu, J. Alloys Compd. **312**, 4 (2000).
[31]P. Blaha, K. Schwarz, G. K. H. Madsen, D. Kvasnicka, and J. Luitz, Wien2k: An augmented plane wave + local orbitals program for calculating crystal properties, Karlheinz Schwarz, Techn. Universität Wien, Austria, 2001.
[32]J. L. Shay, B. Tell, H. M. Kasper, and L. M. Schiavone, Phys. Rev. B **5**, 5003 (1972).
[33]S. Shirakata, S. Chichibu, and S. Isomura, Jpn. J. Appl. Phys., Part 1 **36**, 7160 (1997).
[34]F. H. Allen, Acta Crystallogr., Sect. B: Struct. Sci. **58**, 380 (2002).
[35]S. Chichibu, H. Nakanishi, S. Shirakata, S. Isomura, Y. Harada, S. Matsumoto, H. Higuchi, and T. Kariya, J. Appl. Phys. **80**, 3338 (1996).
[36]J. Paier, R. Asahi, A. Nagoya, and G. Kresse, Phys. Rev. B **79**, 115126 (2009).
[37]G. A. Baraff, Phys. Rev. **128**, 2507 (1962).
[38]B. K. Ridley, J. Phys. C **16**, 3373 (1983).
[39]M. G. Burt, J. Phys. C **18**, L477 (1985).
[40]J. Bude and K. Hess, J. Appl. Phys. **72**, 3554 (1992).
[41]A. Darbandi and O. Rubel, "Impact ionization threshold energy of trigonal selenium: An ab initio study," Can. J. Phys. DOI: 10.1139/cjp-2012-0474 (published online).
[42]C. L. Anderson and C. R. Crowell, Phys. Rev. B **5**, 2267 (1972).
[43]W. Honeyman, J. Phys. Chem. Solids **30**, 1935 (1969).
[44]Y. Morita and T. Narusawa, Jpn. J. Appl. Phys., Part 2 **30**, L1238 (1991).
[45]S. Chichibu, M. Shishikura, J. Ino, and S. Matsumoto, J. Appl. Phys. **70**, 1648 (1991).
[46]S. H. You, K. J. Hong, T. S. Jeong, S. Y. Lee, J. J. Bang, J. D. Moon, and H. S. Kim, J. Cryst. Growth **290**, 18 (2006).
[47]E. M. Conwell, *High Field Transport in Semiconductors, Solid State Physics: Advances in Research and Applications* (Academic Press, New York/London, 1967).
[48]A. M. Andriesh, N. N. Syrbu, M. S. Iovu, and V. E. Tazlavan, Phys. Status Solidi B **187**, 83 (1995).
[49]R. Pässler, J. Appl. Phys. **101**, 093513 (2007).

[50]S. M. Sze and K. K. Ng, *Physics of Semiconductor Devices*, 3rd ed. (John Wiley & Sons, Hoboken, New Jersey, 2007).
[51]L. Y. Sun, L. L. Kazmerski, A. H. Clark, P. J. Ireland, and D. W. Morton, J. Vac. Sci. Technol. **15**, 265 (1978).
[52]L. Roa, J. C. Chervin, A. Chevy, M. Davila, P. Grima, and J. Gonzáez, Phys. Status Solidi B **198**, 99 (1996).
[53]M. I. Alonso, M. Garriga, C. A. D. Rincón, and M. León, J. Appl. Phys. **88**, 5796 (2000).
[54]Y. B. K. Reddy and V. S. Raja, Mater. Chem. Phys. **100**, 152 (2006).
[55]F.-Q. Huang, M.-L. Liu, and C. Yang, Sol. Energy Mater. Sol. Cells **95**, 2924 (2011).
[56]J. H. Schön, J. Oestreich, O. Schenker, H. Riazi-Nejad, M. Klenk, N. Fabre, E. Arushanov, and E. Bucher, Appl. Phys. Lett. **75**, 2969 (1999).
[57]B. Tell, J. L. Shay, and H. M. Kasper, J. Appl. Phys. **43**, 2469 (1972).
[58]L. Barkat, M. Morsli, C. Amory, S. Marsillac, A. Khelil, J. Bernede, and C. El Moctar, Thin Solid Films **431**, 99 (2003).
[59]S. Schuler, S. Siebentritt, S. Nishiwaki, N. Rega, J. Beckmann, S. Brehme, and M. C. Lux-Steiner, Phys. Rev. B **69**, 045210 (2004).
[60]C. L. Bailey, L. Liborio, G. Mallia, S. Tomić, and N. M. Harrison, Phys. Rev. B **81**, 205214 (2010).
[61]K. Hara, T. Shinozawa, J. Yoshino, and H. Kukimoto, J. Cryst. Growth **93**, 771 (1988).
[62]S. Chichibu, S. Shirakata, A. Iwai, S. Matsumoto, H. Higuchi, and S. Isomura, J. Cryst. Growth **131**, 551 (1993).
[63]S. Chichibu, Y. Harada, M. Sugiyama, and H. Nakanishi, J. Phys. Chem. Solids **64**, 1481 (2003).
[64]J. P. Perdew and Y. Wang, Phys. Rev. B **45**, 13244 (1992).
[65]H. J. Monkhorst and J. D. Pack, Phys. Rev. B **13**, 5188 (1976).
[66]J. P. Perdew, Int. J. Quantum Chem. **28**, 497 (1985).
[67]H. Hahn, G. Frank, W. Klingler, A. Meyer, and G. Storger, Z. Anorg. Chem. **271**, 153 (1953).
[68]W. N. Honeyman and K. H. Wilkinson, J. Phys. D: Appl. Phys. **4**, 1182 (1971).